Synthesis and luminescence properties of $Sr_3GdNa(PO_4)_3F$: Sm^{3+} phosphor

Liu Han · Denghui Xu · Qiguang Xu ·
Qiumei Di · Jiayue Sun

Abstract A series of $Sr_3Gd_{(1−x)}Sm_xNa(PO_4)_3F$ (x = 0.01, 0.03, 0.05, 0.07, 0.09) phosphors were synthesized through a conventional high-temperature solid-state reaction. The excitation and emission spectra indicate that these phosphors can be efficiently excited in the range from 350 to 430 nm which matches perfectly with the near-UV light, and emit orange–red light with CIE coordinates (0.5811, 0.4181). The concentration quenching mechanism of Sm^{3+} ions was ascribed to the dipole–dipole interaction. The activation energy E for thermal quenching is calculated to be 0.242 eV. And the lifetime of the $Sr_3Gd_{(1−x)}$ $Sm_xNa(PO_4)_3F$ (x = 0.03, 0.05, 0.07, 0.09) phosphor was determined to be 0.8669, 0.8643, 0.8525, 0.8232 ms, respectively. These orange–red-emitting phosphors might be promising for use in n-UV white LEDs.

Introduction

The past decade has seen a rapid evolution of solid-state lighting sources. White light-emitting diodes (w-LEDs) have many merits such as high efficiency, long lifetime, significant power-saving capability, and environmental friendliness compared with both traditional incandescent and currently implemented fluorescent lamps [1]. Therefore, White light-emitting diodes (w-LEDs) have become another trend for general illumination and have attracted much attention [2, 3]. The most common fabrication technique is by combing an InGaN-based blue diode and yellow phosphor materials [4]. At present, the commercial yellow phosphor can be generated using a blue InGaN LED chip in combination with a yellow phosphor of cerium (III)-doped yttrium aluminum garnet (YAG:Ce^{3+}) [5]. Unfortunately, it exhibits some deficiencies such as high correlated color temperature (CCT > 4500 K) and poor color rendering index (CRI < 80) due to the absence of the red emission [6, 7]. Therefore, to explore high-quality red phosphors with high efficiency, high rendering index, and low CCT is one of the main direction of research and development of practical white LED. An approach to work out this problem is combing a near-ultraviolet (n-UV) emitting LED with a tricolor (blue, green, and red) emitting phosphors when making LEDs, which exhibits excellent color rendering index and an adjustable correlated color temperature [8]. In recent years, the researches of blue and green phosphors which apply to w-LED have been relatively mature [9]. Accordingly, it is an urgent task to explore a high-efficient red-emitting phosphor which can be efficiently excited by the n-UV LED (350–420 nm) chips.

It is well known that Sm^{3+} ion is an important emitting activator because of the stronger absorption of n-UV region [10, 11]. It exhibits high quantum efficiency and produces reddish-orange light emitted due to its 4f-f transitions which has attracted extensive research [12, 13]. Phosphors based on fluorophosphates have many excellent properties, for instance strong visible luminescence, low sintering temperature synthesis, and high chemical stability which have attracted great attention in recent years [14, 15]. And it has a general formula, that is $R_{10}[PO_4]_6Z_2$ and the structure, isotypic with $Ca_{10}(PO_4)_6F_2$ which has been determined by Naray-Szabo [16]. Recently, You et al. reported the luminescence properties of $Sr_3GdNa(PO_4)_3F$: Eu^{2+}, Tb^{3+} phosphors and in this paper, the structure of $Sr_3GdNa(PO_4)_3F$ was determined [17]. According to this,

L. Han · D. Xu · Q. Xu · Q. Di · J. Sun (✉)
School of Science, Beijing Technology and Business University, Beijing 100048, China
e-mail: jiayue_sun@126.com

we synthesized a series of $Sr_3GdNa(PO_4)_3F$: Sm^{3+} phosphors to act as a novel red-emitting phosphor and the luminescence properties were investigated in detail.

Experimental

A series of samples of $Sr_3Gd_{(1-x)}Sm_xNa(PO_4)_3F$ (SGNP: xSm^{3+}, $x = 0.01, 0.03, 0.05, 0.07, 0.09$) were synthesized through a conventional high-temperature solid-state reaction. The raw materials, $SrCO_3$ (AR), NaF (AR), Gd_2O_3 (AR), Sm_2O (99.9 %) $(NH_4)_2HPO_4$ (AR) were weighed stoichiometrically with 15 % excess of NaF and ground evenly in agate mortar. Then the ground powder was firstly sintered at 600 °C for 3 h in crucibles, and then at 1000 °C for 3 h under a reductive atmosphere. After calcining, finally the sample was ground thoroughly into powder for subsequent measurement after being cooled down to room temperature in the furnace.

The phase structure of the samples were performed by X-ray powder diffraction (XRD) in a Bruker-D2 Phase (Cu Kα radiation, 30 kV, 20 mA), and the recorded range of 2θ is from 10° to 80° with a scan rate of 0.08°/s. The photoluminescence (PL) spectra and emission (PL) were measured using a Hitachi F-7000 fluorescence spectrophotometer with a 150 W xenon lamp used as the excitation source. The temperature-dependent photoluminescence properties spectra and luminescent decay curves were recorded on FluoroLog-3 spectrofluorometer (HORIBA, USA), which were combined with the heating apparatus (TAP-02) and a R928P photomultiplier for signal detection, and the Nano LED (N-370) acts as the excitation source when luminescent decay curves were measured.

Results and discussion

Figure 1 shows the X-ray diffraction (XRD) patterns of the prepared phosphors together with the JCPDS card no. 50-1595. According to the recent report by You et al. [17], the standard data of $Sr_3(La,Ce)Na(PO_4)_3(F,OH)$ (JCPDS 50-1595) can be indexed to the X-ray diffraction (XRD) patterns of the prepared phosphors because of all the diffraction peaks of the powder agreeing well with the standard JCPDS card no. 50-1595 and no impurity phase is presented. Therefore, the pure samples were carried out and a few of Sm^{3+} ions were doped into matrix, which do not cause any significant change on the phase formation.

Figure 2 depicts the photoluminescence performances of $Sr_3Gd_{(1-x)}Sm_xNa(PO_4)_3F$ $(x = 0.05)$ phosphor at room temperature. Several excitation peaks can be observed when monitoring at 598 nm which are located at 345 nm $(^6H_{5/2} \rightarrow {}^4H_{9/2})$, 362 nm $(^6H_{5/2} \rightarrow {}^4D_{3/2})$, 374 nm
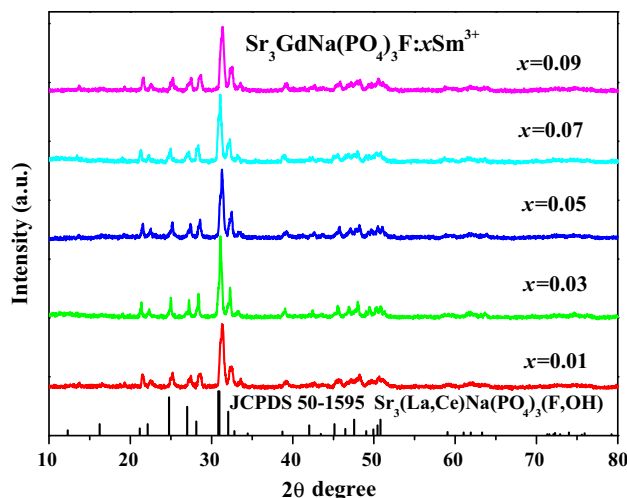
Fig. 1 X-ray diffraction patterns of $Sr_3Gd_{(1-x)}Sm_xNa(PO_4)_3F$ ($x = 0.01, 0.03, 0.05, 0.07, 0.09$) phosphors and the standard data for $Sr_3(La,Ce)Na(PO_4)_3(F,OH)$ JCPDS card no. 50-1595 as a reference
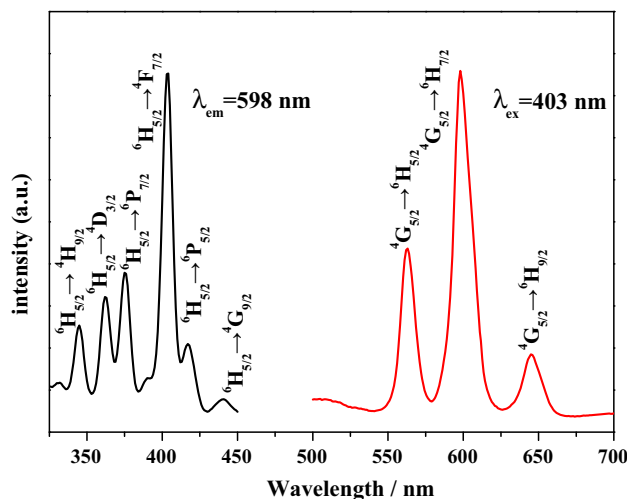
Fig. 2 Excitation and emission spectra of typical $Sr_3Gd_{(1-x)}Sm_xNa(PO_4)_3F$ ($x = 0.05$) phosphor at room temperature

$(^6H_{5/2} \rightarrow {}^6P_{7/2})$, 403 nm $(^6H_{5/2} \rightarrow {}^4F_{7/2})$, 417 nm $(^6H_{5/2} \rightarrow {}^6P_{5/2})$, 442 nm $(^6H_{5/2} \rightarrow {}^4G_{5/2})$ from the perspective and they are attributed to the f → f forbidden transitions of Sm^{3+} [12, 18]. Among them, the highest intensity of transition was centered at 403 nm evidently. And as shown in Fig. 3, we can see the distinct absorption band being centered around 403 nm in the region from 350 to 410 nm of the diffuse reflectance spectrum of $Sr_3GdNa(PO_4)_3F$ and $Sr_3Gd_{(1-x)}Sm_xNa(PO_4)_3F$ ($x = 0.01, 0.03, 0.05, 0.07, 0.09$). These findings indicate that the prepared phosphor can be effectively excited by near-UV LED chips (350–420 nm), which is significant for the fabrication of near-UV chips in w-LEDs. There are three emission peaks in the emission
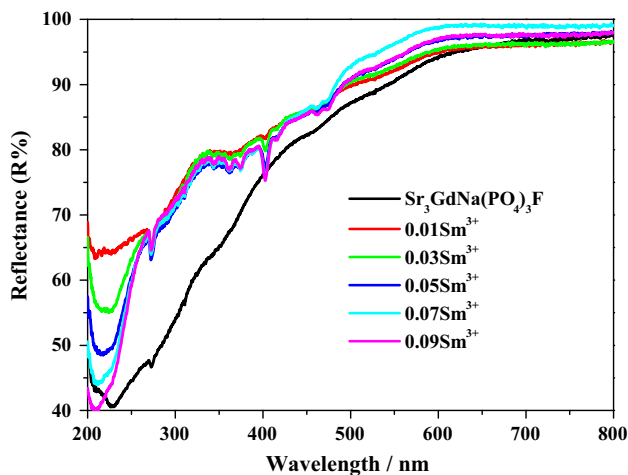
Fig. 3 UV-Vis diffuse reflectance spectra of $Sr_3GdNa(PO_4)_3F$ and $Sr_3Gd_{(1-x)}Sm_xNa(PO_4)_3F$ ($x = 0.01, 0.03, 0.05, 0.07, 0.09$)

Fig. 4 CIE chromaticity diagram for $Sr_3Gd_{0.95}Sm_{0.05}Na(PO_4)_3F$ phosphor

Fig. 5 Emission spectra of $Sr_3Gd_{(1-x)}Sm_xNa(PO_4)_3F$ ($x = 0.01, 0.03, 0.05, 0.07, 0.09$) at room temperature ($\lambda_{ex} = 403$ nm)

spectrum located around 563, 598, and 646 nm, which correspond with $^4G_{5/2} \rightarrow {}^6H_J$ ($J = 5/2, 7/2$, and $9/2$) transitions when excited at 403 nm. And to the best of our knowledge, the $^4G_{5/2} \rightarrow {}^6H_{5/2}$ (563 nm) mainly obeys the magnetic-dipole transition (MD), the $^4G_{5/2} \rightarrow {}^6H_{7/2}$ (598 nm) is a partly magnetic dipole and partly electric-dipole transition (ED), the $^4G_{5/2} \rightarrow {}^6H_{9/2}$ (646 nm) originates from purely ED transition [12, 19]. It is believed that the intensity of $^4G_{5/2} \rightarrow {}^6H_{7/2}$ (598 nm) is the highest of three transitions. Furthermore, the CIE 1931 chromaticity of $Sr_3Gd_{0.95}Sm_{0.05}Na(PO_4)_3F$ phosphor under 403 nm excitation is calculated to be (0.5811, 0.4181), as shown in Fig. 4. All of these results indicate that the prepared phosphor can be applied to orange–red-emitting phosphor.

Figure 5 shows the emission intensities of $Sr_3Gd_{(1-x)}Sm_xNa(PO_4)_3F$ at different doping concentrations of Sm^{3+} ions ($x = 0.01, 0.03, 0.05, 0.07, 0.09$) at room temperature ($\lambda_{ex} = 403$ nm). It can be seen that the emission intensity of $Sr_3Gd_{(1-x)}Sm_xNa(PO_4)_3F$ increases initially with the rising concentration of Sm^{3+} ions then decreases and achieves the maximum when $x = 0.05$ due to the occurrence of the concentration quenching, as shown in the inset.. Consequently, the optimum concentration of Sm^{3+} is determined to be about 0.05. The behavior of concentration quenching is mainly generated by the process of nonradiative energy migration among the Sm^{3+} ions at the high concentration. And the concentration quenching mechanism is ascribed to two main aspects: one is multipolar interaction and the other is exchange interaction [20]. The critical transfer distance between donor and acceptor should be shorter than 0.5 nm if the energy transfer due to the exchange interaction. Accordingly, in order to confirm the concentration quenching mechanism of phosphor, the calculation of the critical
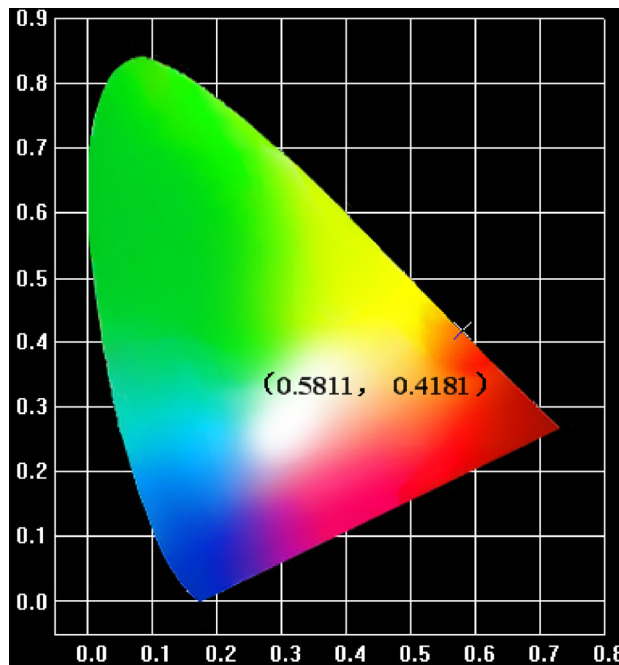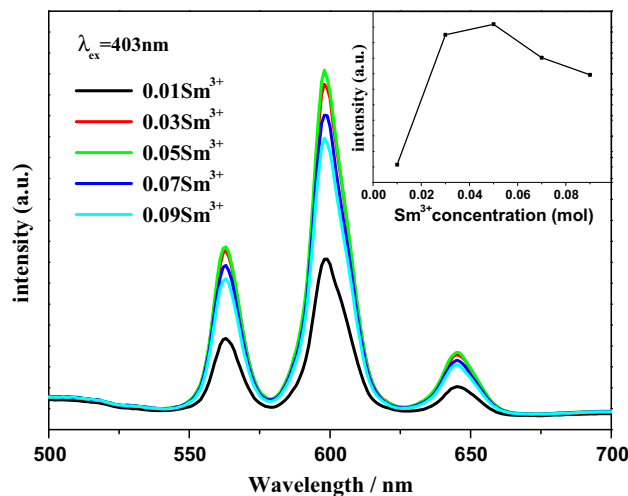
distance (R_c) is essential. According to Blasse's theory, the critical distance (R_c) between the Sm^{3+} ions can be calculated using the following equation [21]

$$R_c = 2\left[\frac{3V}{4\pi x_c N}\right]^{1/3}, \tag{1}$$

where V is the volume of the unit cell, N represents the number of Sm^{3+} ions in the $Sr_3GdNa(PO_4)_3F$ unit cell, x_c is the critical concentration. For $Sr_3GdNa(PO_4)_3F$ host,
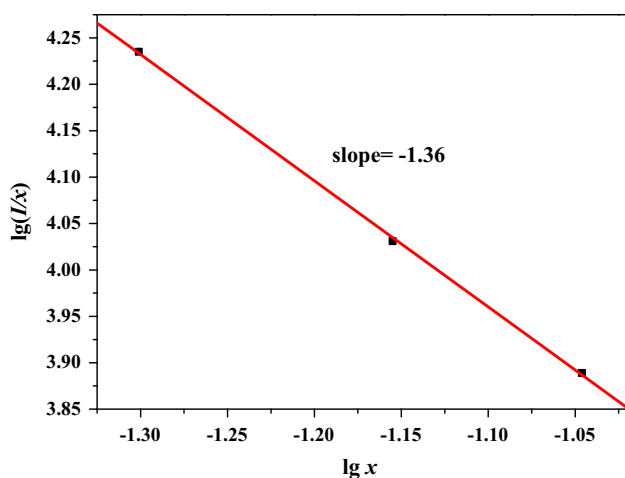
Fig. 6 Curve of lg (I/x) versus lgx in $Sr_3Gd_{(1-x)}Sm_xNa(PO_4)_3F$ ($x = 0.05, 0.07, 0.09$) phosphors

Fig. 7 Emission spectra of $Sr_3Gd_{0.95}Sm_{0.05}Na(PO_4)_3F$ phosphor for various temperatures excited at 403 nm; the inset shows temperature-dependent relative emission intensity of $Sr_3Gd_{0.95}Sm_{0.05}Na(PO_4)_3F$ phosphor

$N = 2$, $V = 56.4795$ nm^3, $x_c = 0.05$, therefore, the value of the critical transfer distance R_c for Sm^{3+} is calculated to be 5.1287 nm. Obviously, the value calculated is much larger than 0.5 nm. Therefore, the concentration quenching among the Sm^{3+} ions in the phosphor is ascribed to the multipolar interaction. On the basis of Dexter's theory, the energy transfer expressions of multipolar interaction can be divided into dipole–dipole, dipole–quadrupole, and quadrupole–quadrupole interactions. Furthermore, according to Van Uiter's report, the emission intensity (I) per activator ion follows the equation [22]:

$$\frac{I}{x} = K \left[1 + \beta \left(x \right)^{\theta/3} \right]^{-1}, \quad (2)$$

where x is the activator concentration, I/x is the emission intensity per activator concentration, k and β are constants for a given host crystal in the same excitation condition, $\theta = 6$, 8, and 10 represent dipole–dipole, dipole–quadrupole, and quadrupole–quadrupole interactions, respectively. The Eq. (3) can be obtained by means of taking the Eq. (2) to the form of logarithm.

$$\lg \left(\frac{I}{x} \right) = C - \frac{\theta}{3} \lg x \quad (3)$$

In order to acquire the value of θ, choosing $x = 0.05$, 0.07, 0.09 and its corresponding emission intensity, respectively. The dependence of lg (I/x) on lg x plotted is shown in Fig. 6. Therefore, the value of θ was calculated to be 4.08, which is approximate to 6, namely, the pattern of energy transfer is dipole–dipole. For more clarity, the concentration quenching of Sm^{3+}ions was ascribed to the dipole–dipole interaction.

Figure 7 shows the emission spectra of $Sr_3Gd_{0.95}Sm_{0.05}$ $Na(PO_4)_3F$ phosphor for various temperatures excited at 403 nm; the inset shows temperature-dependent relative
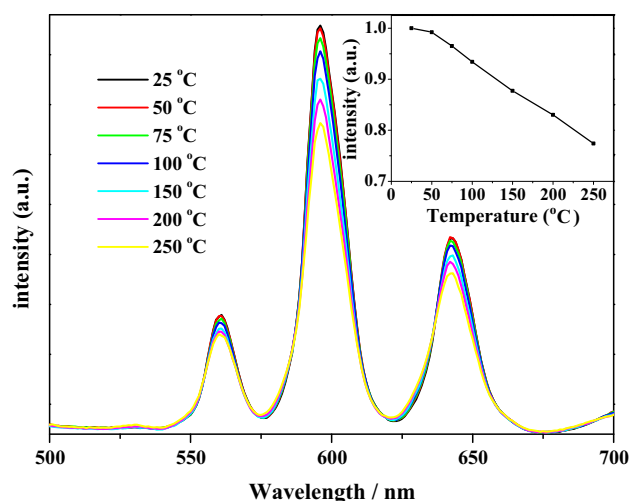
emission intensity of $Sr_3Gd_{0.95}Sm_{0.05}Na(PO_4)_3F$ phosphor. The integrated emission intensity of $Sr_3Gd_{0.95}$ $Sm_{0.05}Na(PO_4)_3F$ phosphor sustainably decreases with increasing temperature between from 25 to 250 °C with excitation at 403 nm, which is partly due to the thermal quenching in the configurational coordinate diagram [5]. Firstly, the luminescence center of excited state is thermally activated by the means of phonon interaction and then releases through the crossing point between the excited state and the ground state in the configurational coordinate diagram, finally bringing about the luminescence quenching [7]. The clarification of thermal quenching behavior and the value of activation energy can be achieved through the Arrhenius equation [23] :

$$I(T) \approx \frac{I_0}{1 + c \exp\left(-\frac{E}{kT}\right)}, \quad (4)$$

where I_0 is the first luminescence intensity and $I(T)$ is the luminescence intensity of Sm^{3+} in the presence of temperature, k is Boltzmann's constant (8.617×10^{-5} eV/K), and c is a constant, E is the activation energy for thermal quenching. The value of E can be estimated through the Eq. (5) which is rearranged by the Eq. (4) as follows:

$$\ln \left[\left(\frac{I_0}{I} \right) - 1 \right] = -\frac{E}{kT} + \ln c \quad (5)$$

Figure 8 shows the plots of ln [(I_0/I)−1] versus 1/kT for $Sr_3Gd_{0.95}Sm_{0.05}Na(PO_4)_3F$ phosphor. Accordingly, the activation energy E for thermal quenching is calculated to be 0.242 eV. Thus the thermal quenching of prepared phosphors was small, which was required when used in w-LEDs. Additionally, the CIE chromaticity coordinate

Fig. 8 The plots of ln $[(I_0/I)-1]$ versus $1/kT$ for $Sr_3Gd_{0.95}$ $Sm_{0.05}Na(PO_4)_3F$ phosphor
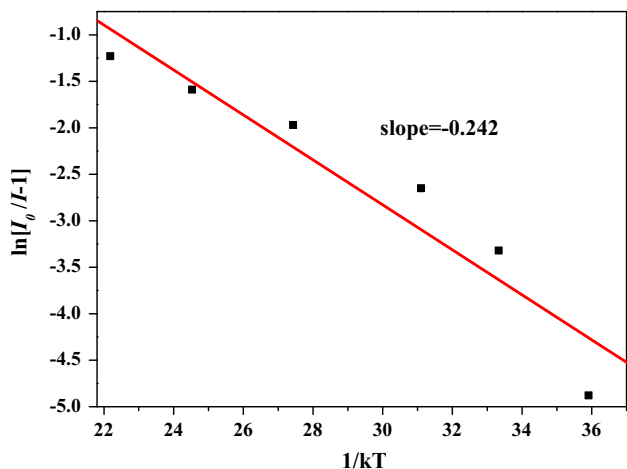
Fig. 9 The decay curve of $Sr_3Gd_{(1-x)}Sm_xNa(PO_4)_3F$ ($x = 0.03$, 0.05, 0.07, 0.09) phosphor

(x, y) of $Sr_3Gd_{0.95}Sm_{0.05}Na(PO_4)_3F$ phosphor at different temperatures respectively are given in Table 1. It is clear that the CIE chromaticity coordinate has a slighter motion with the increscent of temperature so as to keep good color quality. Therefore, the prepared phosphor has a good thermal stability and chemical stability which is significant when it is applied to in w-LEDs.
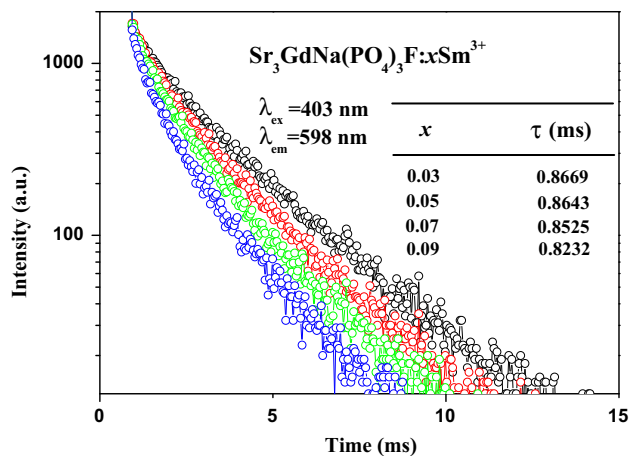
The PL decay curves of $Sr_3Gd_{(1-x)}Sm_xNa(PO_4)_3F$ at different doping concentrations of Sm^{3+} ions ($x = 0.03$, 0.05, 0.07, 0.09) were measured so as to investigate the luminescence dynamics. Figure 8 shows the decay curve of $Sr_3Gd_{(1-x)}Sm_xNa(PO_4)_3F$ ($x = 0.03$, 0.05, 0.07, 0.09) phosphor. And the lifetime can be defined as follows:

$$I = A_1\exp(-t/\tau_1) + A_2\exp(-t/\tau_2), \quad (6)$$

where I is the luminescence intensity at a time t, τ_1 and τ_2 are exponential components of the decay time, A_1 and A_2 are constants. On the basis of Eq. (7) which is rearranged by the Eq. (6), the lifetime of the $Sr_3Gd_{(1-x)}Sm_xNa(PO_4)_3F$ ($x = 0.03$, 0.05, 0.07, 0.09) phosphor were determined to be 0.8669, 0.8643, 0.8525, 0.8232 ms, respectively.

$$\tau = \frac{A1\,\tau_1^2 + A2\,\tau_2^2}{A1\,\tau_1 + A2\,\tau_2} \quad (7)$$

It is clear that the lifetime decreases with increased concentration. According to a spin selection rule, the activator Sm^{3+} ions have a long decay time induced by a forbidden transition of Sm^{3+} which has a very low probability and decay time in the level of ms [6]. Obviously, the lifetime of prepared phosphors are short enough for potential applications in w-LED Fig. 9.

Conclusions

In summary, samples of $Sr_3Gd_{(1-x)}Sm_xNa(PO_4)_3F$ (SGNP: xSm^{3+}, $x = 0.01$, 0.03, 0.05, 0.07, 0.09) were synthesized through a conventional high-temperature solid-state reaction. The photoluminescence properties, temperature-dependent luminescence, and decay times were investigated in detail. The obtained phosphors have a distinct excitation band centered at 403 nm ranging from 350 to 430 nm which can match perfectly with the n-UV LED chips. The CIE 1931 chromaticity of the prepared phosphor under 403 nm excitation was calculated to be (0.5811, 0.4181). And phosphors can emit intense orange–red light with an optimal concentration of 0.05 under the excitation of 403 nm. The concentration quenching is ascribed to dipole–dipole interaction. The prepared phosphor has a good thermal stability and chemical stability. All of these results indicate that the prepared phosphor can be applied to orange–red-emitting n-UV white LEDs.

Table 1 The CIE chromaticity coordinate (x, y) of $Sr_3Gd_{0.95}Sm_{0.05}Na(PO_4)_3F$ phosphor from 25 to 250 °C

	25 °C	50 °C	75 °C	100 °C	150 °C	200 °C	250 °C
CIE (x)	0.5811	0.5810	0.5810	0.5807	0.5800	0.5789	0.5774
CIE (y)	0.4181	0.4182	0.4181	0.4184	0.4192	0.4202	0.4218

References

1. Schubert EF, Kim JK (2005) Solid-state light sources getting smart. Science 308:1274–1278

2. Nakamura SJ, Senoh M, Mukai T (1993) High-power InGaN/GaN double-hetero strructure violet light-emitting-diodes. Appl Phys Lett 62:2390–2392

3. Zhang ZY, Wang JG, Yin YL, Zhou JJ, Zhou SP, Pan YX (2013) A novel green-to-yellow emitting phosphor: $BaSi_2SN_{2.67}:Eu^{2+}$ for potential application in UV-LEDs. Opt Mater 35:1273–1275

4. Xia ZG, Ji JH, Huang ZhH, Atuchin VV (2014) New yellow-emitting whitlockite-type structure $Sr_{1.75}Ca_{1.25}(PO_4)_2$: Eu^{2+} phosphor for near-UV pumped white light-emitting devices. Inorg Chem 53:5129–5135

5. Sun JY, Cui DP (2014) Synthesis, structure, and thermally stable luminescence of Dy^{3+}-doped $Na_3YSi_2O_7$ host compound. J Am Ceram Soc 97:843–847

6. Sun JY, Zhang XY, Xia ZG, Du HY (2012) Luminescent properties of $LiBaPO_4$: RE (RE = Eu^{2+}, Tb^{3+}, Sm^{3+}) phosphors for white light-emitting diodes. J Appl Phys 111:013101–013103

7. Sun JY, Han L, Xu QG, Di QM (2014) Synthesis and luminescence properties of $Na_3YSi_2O_7$: Sm^{3+} phosphor. Ceram Int 40:14261–14265

8. Shang MM, Li GG, Geng DL, Yang DM, Kang XJ, Zhang Y, Lian HZ, Lin J (2012) Blue emitting $Ca_8La_2(PO_4)_6O_2$: Ce^{3+}/Eu^{2+} phosphors with high color purity and brightness for white LED: soft-chemical synthesis, luminescence, and energy transfer properties. J Phys Chem C 116:10222–10231

9. Sun JY, Zeng JH, Sun YN, Du HY (2013) Tunable luminescence of Ce^{3+}/Mn^{2+}-coactivated $Sr_3Gd(PO_4)_3$ with efficient energy transfer for white-light-emitting diode. J Lumin 138:72–76

10. Sun JY, Zeng JH, Sun YN, Du HY (2013) Synthesis and luminescence properties of novel $Y_2Si_4N_6C$: Sm^{3+} carbonitride phosphor. Ceram Int 39:1097–1102

11. Lei BF, Li B, Zhang HR, Li WL (2007) Preparation and luminescence properties of $CaSnO_3$: Sm^{3+} phosphor emitting in the reddish orange region. Opt Mater 29:1491–1494

12. Yu RJ, Jeong JH, Jang K (2014) Photoluminescence characteristics of Sm^{3+} doped $Ba_3La(PO_4)_3$ as new orange-red emitting phosphors. J Lumin 145:717–722

13. Dabre KV, Park K, Dhoble SJ (2014) Synthesis and photoluminescence properties of microcrystalline Sr_2ZnWO_6: RE^{3+} (RE = Eu, Dy, Sm and Pr) phosphors. J Alloy Compd 617:129–134

14. Jiao MM, Guo N, Lü W, Jia YC, Lv WZ, Zhao Q, Shao BQ, You HP (2013) Tunable blue-green-emitting $Ba3LaNa(PO4)3F$: Eu2+, Tb3+ phosphor with energy transfer for near-UV white LEDs. Inorg Chem 52:10340–10346

15. Mi RY, Zhao CL, Xia ZG (2014) Synthesis, structure, and tunable luminescence properties of novel $Ba_3NaLa(PO_4)_3F$: Eu^{2+}, Mn^{2+} phosphors. J Am Ceram Soc 6:1802–1808

16. Mayer I, Roth R, Brown W (1974) Rare earth substituted fluoride-phosphate apatites. J Solid State Chem 11:33–37

17. Jiao MM, Jia YC, Lu W, Lv W, Zhao Q, Shao BQ, You HP (2014) $Sr_3GdNa(PO_4)_3F$: Eu^{2+}, Mn^{2+}: a potential color tunable phosphor for white LEDs. J Mater Chem C 2:90–97

18. Wu MQ, Liu XL, Gu M, Ni C, Liu B, Huang SM (2014) Characterization and luminescence properties of sol-gel derived M'-type $LuTaO_4$: Ln^{3+} (Ln = Pr, Sm, Dy) phosphors. Mater Res Bull 60:652–658

19. Raut SK, Dhoble NS, Park K, Dhoble SJ (2014) Precipitation based synthesis and luminescence of Ln^{3+} (Eu, Ce, Dy, Sm, Tb) activated $BaCa_2Si_3O_9$-Walstromite cyclosilicate phosphors. Mater Chem Phys 147:594–603

20. Xia ZG, Liu RS (2012) Tunable blue-green color emission and energy transfer of $Ca_2Al_3O_6F$: Ce^{3+}, Tb^{3+} phosphors for near-UV white LEDs. J Phys Chem C 116:15604–15609

21. Xia ZG, Zhuang JQ, Liao LB, Liu HK, Luo Y, Du P (2011) Synthesis and luminescence properties of $Ba_2Gd(BO_3)_2Cl$: Eu^{2+} phosphor. J Electrochem Soc 158:J359–J362

22. Zhou J, Xia ZG, Yang MX, Shen K (2012) High efficiency blue emitting phosphor: Ce^{3+}-doped $Ca_{5.45}Li_{3.55}(SiO_4)_3O_{0.45}F_{1.55}$ for near UV pumped light-emitting diodes. J Mater Chem 22:21935–21941

23. Li GG, Geng DL, Shang MM, Zhang Y, Peng C, Cheng ZY, Lin J (2011) Color tuning luminescence of Ce^{3+}/Mn^{2+}/Tb^{3+}-triactivated $Mg_2Y_8(SiO_4)_6O_2$ via energy transfer: potential single-phase white-light-emitting phosphors. J Phys Chem C 115:21882–21892